

Spectroscopy Letters

An International Journal for Rapid Communication

ISSN: (Print) (Online) Journal homepage: https://www.tandfonline.com/loi/lstl20

Raman spectroscopic investigation of the wear effect on the titanium carbonitride/aluminum oxide/titanium nitride coated cutting tool

Sefa Celik, Nuray Bekoz Ullen, Sevim Akyuz & Aysen E. Ozel

To cite this article: Sefa Celik, Nuray Bekoz Ullen, Sevim Akyuz & Aysen E. Ozel (2022) Raman spectroscopic investigation of the wear effect on the titanium carbonitride/aluminum oxide/titanium nitride coated cutting tool, Spectroscopy Letters, 55:3, 172-182, DOI: 10.1080/00387010.2022.2041039

To link to this article: https://doi.org/10.1080/00387010.2022.2041039

Published online: 24 Feb 2022.

Submit your article to this journal

Article views: 81

View related articles

View Crossmark data

Full Terms & Conditions of access and use can be found at
https://www.tandfonline.com/action/journalInformation?journalCode=lstl20

SPECTROSCOPY LETTERS
2022, VOL. 55, NO. 3, 172–182
https://doi.org/10.1080/00387010.2022.2041039

Taylor & Francis
Taylor & Francis Group

Check for updates

Raman spectroscopic investigation of the wear effect on the titanium carbonitride/aluminum oxide/titanium nitride coated cutting tool

Sefa Celik[a], Nuray Bekoz Ullen[b], Sevim Akyuz[c] and Aysen E. Ozel[a]

[a]Department of Physics, Faculty of Science, Istanbul University, Istanbul, Turkey; [b]Department of Metallurgical and Materials Engineering, Faculty of Engineering, Istanbul University-Cerrahpasa, Istanbul, Turkey; [c]Department of Physics, Faculty of Science and Letters, Istanbul Kultur University, Istanbul, Turkey

ABSTRACT

In this study, micro-Raman spectroscopy technique in combination with multivariate statistical analysis was carried out to investigate the worn surfaces and metallurgical changes in the wear land of chemical vapor deposition—applied titanium carbonitride/aluminum oxide/titanium nitride-coated cutting inserts. To understand the wear process, detailed scanning electron microscopy analysis was also performed. The structural change at the molecular level of the coating due to the wear of the cutting-edge layers was investigated. Tool life was determined at 0.5 mm flank wear of the cutting tool. Thirty-four Raman spectra recorded from the different points of the worn parts of nine cutting inserts were investigated in comparison with the seven spectra of the different points of three unused cutting inserts. The principal component analysis followed by linear discriminant analysis performed on 41 Raman spectral data, clearly separated the samples as worn and unworn cutting inserts, and showed the wear effects. The comparison of the mean Raman spectrum of worn and unworn (unused) cutting inserts showed that the intensities of the aluminum oxide and titanium nitride bands were decreased, whereas the titanium carbide band at 672 cm^{-1} was increased, as a result of the wear effect. Moreover, the relative intensity of disordered carbon (D band) band to the graphitic sp^2 bonded carbon (G band) band was found to increase, due to wear.

ARTICLE HISTORY
Received 26 January 2022
Accepted 7 February 2022

KEYWORDS
Chemical vapor deposition; crystalline degree; multivariate statistical analysis; vibrational spectroscopy

Introduction

Machining operations such as turning, milling, and drilling are commonly employed machining processes in industry. The machinability is dependent on the workpiece and tool material characteristics, such as composition expressed in microstructure, mechanical and physical properties, and cutting conditions and machining parameters, such as tool material and tool geometry. In order to select the right tool and machining parameters, knowledge of the loads on the tool and the properties of the tool material is necessary, together with an analysis of the wear mechanisms, which should be characterized in more detail for the machining process, and their interaction.[1–4] Recent studies in the machining have shown that the cutting insert selection has a major influence on the properties of finished parts.[5–7] This study contains the results of the cutting tool wear mechanisms.

In many technical fields, high-strength steels like AISI 4140 (42CrMo4 + QT) are commonly used for highly dynamically loaded parts in plant engineering or engine components. The AISI 4140 steel is one of the representative medium carbon and low alloy steels that have been used for a wide utility. Increasing demands on weight, performance, and efficiency of the automotive industry led to increasing demands on material properties.[8–10] Tool wear is the most important and decisive factor for successfully maximizing the production process and automation in any typical metal cutting operation. Therefore, tool wear monitoring is an essential requirement for the realization of automated production. Much research has been conducted to characterize the tool wear behaviors of AISI 4140 steel, worked under different machining and processes conditions.[8–13] The objective of in this study is to

CONTACT Sefa Celik scelik@istanbul.edu.tr Department of Physics, Faculty of Science, Istanbul University, Vezneciler 34134, Istanbul, Turkey.
© 2022 Taylor & Francis Group, LLC

examine the wear behavior of chemical vapor deposition (CVD) TiCN/Al2O3/TiN-coated cutting insert during turning on AISI 4140 steel.

The cutting tools wear as using, due to reasons such as adhesion, diffusion, thermal softening, oxidation, micro-chipping, and fatigue.[14] The flank wear of cutting tools is often chosen as the tool life criterion as it determines the diametrical accuracy, stability, and reliability of the machining.[12] The TiCN coatings on cutting tools, made by CVD, have important properties such as excellent adherence, high hardness, and high durability. Although titanium carbonitride coatings provide good protection against surface wear, its deterioration is due to the formation of titanium oxide on surfaces causing delamination.[15] TiAlN coatings are widely used as they show oxidation resistance up to 750 °C. Tool wear is one of the most critical problems in machining. Wear is caused by rapidly moving chips on the tool wear surfaces and the high normal loads exerted by the workpiece. In addition, the associated friction on these contacting surfaces increases with temperature, further accelerating tool wear. Chemical vapor deposited in end coatings has attracted great attention in recent years for cutting tool applications, including rotary tools and inserts, due to its excellent physical and chemical properties.[16]

Micro-Raman spectroscopy, along with all vibrational spectroscopic techniques, is a valuable noninvasive analytical technique that provides vibrational information about organic and inorganic molecules. This technique has also been used in the field of surface engineering to examine to study the effect on coatings due to wear and wear residues.[17–25] Vancoille et al.[18] have studied tribo-oxidation of a TiN coating sliding against corundum, using micro-Raman spectroscopy together with transmission electron microscopy, and concluded that the structure of debris depended on the sliding speed. Raman spectroscopic analysis indicated that the wear debris, formed at the low and medium sliding speed, consisted of both anatase and rutile nanocrystalline structural elements of TiO_2 whereas, only rutile was formed in the debris formed at the high sliding speed. The Raman piezo-spectroscopic behavior of aluminum nitride was investigated by Murari et al.,[19] and the Raman spectral shift induced by stress was determined. It was concluded that Raman spectroscopy gave valuable information regarding the structural damage of the material close to the surface. The laser-induced oxidation of transition-metal borides, carbides, and nitrides, including TiN and TiC powders, during Raman micro-spectroscopic analysis was reported by Begun and Bamberger.[20] In this study, the formation of surface oxides due to laser heating was revealed. Also, the structural characterization of TiN coatings oxidized by solar beam heat treatment[21] and TiN films grown on silicon substrates by pulsed laser deposition[22] were performed by Raman spectroscopy. Constable et al.[23] performed Raman spectroscopic investigations on a series of Physical Vapor Deposition (PVD) ceramic hard coatings, deposited on steel substrates using the cathodic arc/unbalanced magnetron deposition technique and reported the wavenumbers of the optic and acoustic phonon modes of the TiN, ZrN, TiAlN, TiZrN, and TiCN coatings. In this study, it was concluded that Raman micro-spectroscopy has been a very useful nondestructive technique for characterization of PVD hard coatings. Badiger et al.[24] investigated the tribological behavior of TiC-C monolayer and Ti/TiN/TiCN/TiN/TiCN multilayer coatings. In this study, Field Emission Scanning Electron Microscopy (FESEM) - Energy Dispersive Spectroscopy (EDS), Raman spectroscopy, optical profiler, and confocal microscope techniques were used for characterization of coatings and investigation the wear behavior. The titanium-based multilayered hard coatings developed on the highly alloyed steel MDN121 by cathodic arc evaporation technique were investigated by Raman spectroscopy, and the coating structure was confirmed by the presence of diamond-like-carbon, TiN, and TiN Raman peaks.[25]

In this study, the structural change of the CVD TiCN/Al_2O_3/TiN-coated cutting insert, due to wear, was investigated using Raman spectroscopy. For this purpose, 41 Raman spectra were investigated. Thirty-four spectra from the different points of the worn parts of the nine used cutting inserts coated with TiCN/Al_2O_3/TiN and the seven spectra from the different points of three unused cutting inserts were comparatively analyzed. Multivariate statistical analysis (principal

Table 1. Chemical composition of AISI 4140 material, machined with the titanium carbonitride/ aluminum oxide/ titanium nitride coated cutting insert.

Elements	C	Mn	Si	Cr	S	P	Mo	Fe
Weight, %	0.42	0.80	0.20	0.85	0.025	0.025	0.18	Bal.[a]

[a]Bal: balance.

component analysis [PCA] and linear discriminant analysis [LDA]) was performed to determine at molecular level similarities and dissimilarities of the unworn and worn parts of the TiCN/Al_2O_3/TiN-coated cutting inserts. In addition, scanning electron microscopy (SEM) has been used to study the wear behavior of cutting insert.

Materials and methods

Experimental details

In this study, machining of the workpiece materials was carried out in form of turning operation. The AISI 4140 steel [quenched and tempered up to hardness of 58 Hardness (HRC)] was preferred as workpiece material for evaluating the performance of selected cutting tool. The workpiece is 50 mm in diameter, and it is hardened to 55 HRC. The chemical composition of this AISI 4140 material, machined with the TiCN/Al_2O_3/TiN-coated cutting insert is given in Table 1.

The turning tests were conducted on YouJi Machine Industrial Co. Ltd. production CNC lathe machine with X and Z axes, at 550 mm machining volume and 3000 rpm. All machinability tests were performed in a dry cutting condition without any coolant. All the cutting parameters were kept constant. Cutting parameters were determined as 150 m/min of cutting speed, 0.1 mm/rev of feed rate and 0.5 mm of cutting depth. Tool holder is codified as PSBNR 25 × 25 K12 with a common active part tool geometry described by 75 degrees (setting angle), −6 degrees (reke angle), and −5 degrees (clearance angle).

The tool holder with an adjustable three-dimensional mechanism was fixed on the rotary B-axis table. Cutting tools were placed on the tool holder; thus, the tool can be moved in the X-axis direction and also be rotated about the B-axis. The properties of the TiCN/Al_2O_3/TiN multilayered-coated cutting tool insert produced by Sandvik Coromant Company[26] are given in

Table 2. The properties of the titanium carbonitride/aluminum oxide/titanium nitride cutting tool insert.[26]

Tool material	WNMG-080408 MKS WKK 10 S
Chemical compositions	30%TiCN + 50% Al_2O_3 + %20 TiN
Coating thickness	2 μm
Hardness	2700–2900 HV

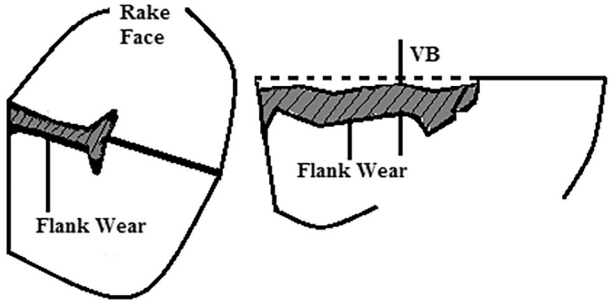

Figure 1. Schematic of flank wear region on the titanium carbonitride/aluminum oxide/titanium nitride-coated cutting insert. The flank wear criterion (VB) is indicated.

Table 2. Cutting insert used in this research is CVD type because it is the most used coated inserts in metal cutting today. In the turning test, only one cutting edge is used in each experiment. The flank wear of the cutting insert was studied during turning of the AISI 4140 steels. Fig. 1 is shown land width as known flank wear criterion (VB) and flank wear pattern of TiCN/Al_2O_3/TiN-coated cutting insert.

The wear characterization of the cutting tool insert was performed using a scanning electron microscopy (SEM) at different magnifications (Quanta FEG450 model).

The Raman spectra of the samples were recorded using a JASCO NRS-3100 model dispersive micro-Raman spectrometer (1200 lines/mm grating and high-sensitivity cooled charged-coupled device). The spectrometer was calibrated with the silicon phonon mode at 520 cm^{-1} and 532 nm green laser diode was used for excitation with the exposure time was taken as 2 s, and 100 spectra were accumulated. The GRAMS/AI 7.02 (Thermo Electron Corporation, Waltham, MA) software package was used to perform a comprehensive processing.

To determine the similarities and dissimilarities of the unworn and worn parts of the TiCN/Al_2O_3/TiN-coated cutting inserts, multivariate statistical analysis is needed. For this purpose, a combination of both unsupervised and supervised algorithms were applied.[27] PCA can be used as an unsupervised algorithm

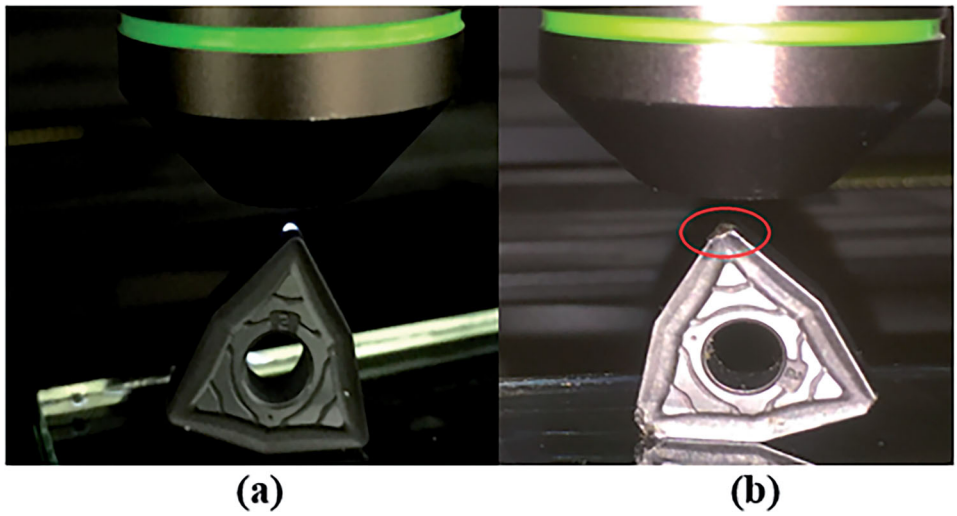

Figure 2. View of cutting tips of titanium carbonitride/aluminum oxide/titanium nitride-coated cutting insert before (a) and after (b) wear.

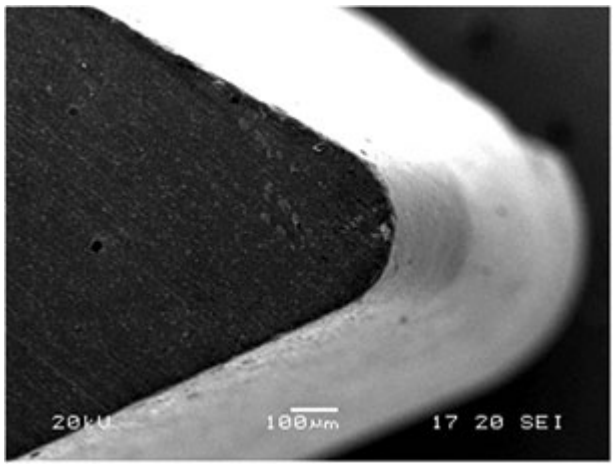

Figure 3. Scanning electron microscopy image of unused titanium carbonitride/aluminum oxide/titanium nitride-coated cutting insert (scale bar: 100 µm; acceleration voltage 20 kV).

for a data reduction purposes. It minimizes the variance within classes, to account for heterogeneity of similar samples. However, a supervised algorithm such as LDA maximizes the variance between classes, allowing for diagnostic differences to be noticed. For this reason, LDA is performed by following the PCA results, to maximize the variance between classes and to allow the distinctive differences to be determined. PCA-LDA analysis was conducted using the IRootlab toolbox[28] for MATLAB.

Result and discussion

In this study, nine used and three unused cutting inserts coated with TiCN/Al_2O_3/TiN CVD were

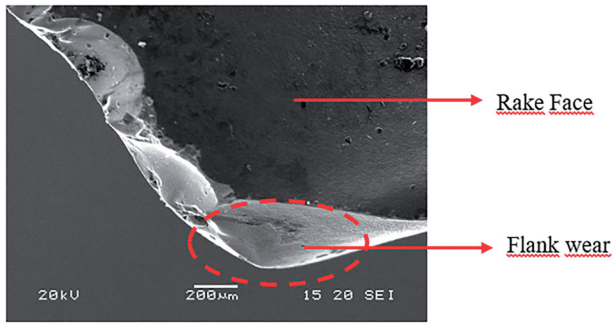

Figure 4. Scanning electron microscopy image of worn titanium carbonitride/aluminum oxide/titanium nitride-coated cutting tool after machining (scale bar: 200 µm; acceleration voltage 20 kV).

investigated. The appearance of the cutting tips before and after wear is shown in Fig. 2.

Tool wear results

To better interpret the images; Fig. 3 shows the SEM image of the unused multilayered-coated cutting insert. For machining AISI 4140 steel alloy, SEM images of the flank wear are shown in Fig. 4 to demonstrate the failure mechanisms of multilayered (TiCN/Al_2O_3/TiN)-coated insert. As clearly seen in the Fig. 4, the tool life was determined in approximately 2.5 min with a side wear area of approximately 0.5 mm resulting from coating defects. The side wear area is even and uniform, indicating that tool wear is a steady and gradual process. As mentioned in many studies, tool wear during turning occurs mainly on the

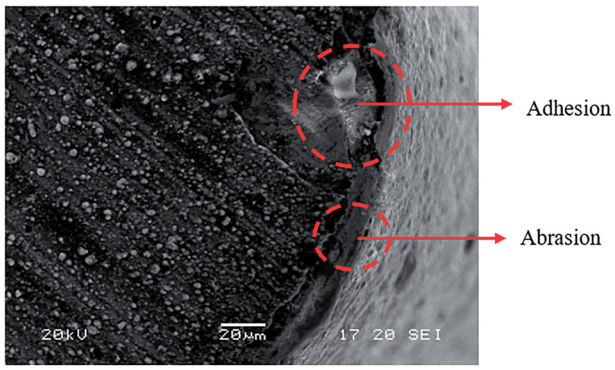

Figure 5. Scanning electron microscopy image of the abrasion and adhesion wear mechanisms on the flank face of the worn titanium carbonitride/aluminum oxide/titanium nitride-coated cutting tool.

rake face and flank of the cutting tool.[8,29] Flank wear is a common phenomenon in metal cutting that causes significant economic losses from material loss and machine downtime. Various monitoring techniques are used to detect flank wear.[30,31] The SEM examination we used in our study is the most common.

The wear occurs mainly at the flank location during the turning operation. This is supported by many studies on the various machining[29–32]. SEM image in Fig. 5 and the adhesion and abrasion wear mechanisms on the flank face are clearly observed. Both wear marks are clear on the all cutting tool flanks used in the study. The wear mechanisms that occur on the cutting tool during the processing of steel alloys are abrasive wear, adhesive wear, diffusion wear, oxidation wear, and so on, that occur under various conditions.[1]

Raman spectral results

In this study, 41 Raman spectra were investigated. Thirty-four spectra from the different points of the worn parts of the nine used and the seven spectra from the different points of three unused cutting inserts were comparatively analyzed. The obtained Raman spectral data were pretreated before analysis, rubberband baseline correction and vector normalization preprocesses were applied, respectively.[33] For the rubberband baseline correction technique, the spectrum is divided into (N) ranges and the lowest points in every range are determined. These minima points of the spectral region are used to fit a convex polygonal line (rubberband), which is then subtracted from the original spectrum.[33] To make the spectral differences more pronounced, we averaged the spectra of each group. The mean of the 34 spectra taken from the worn parts of the used cutting inserts, together with the mean of the 7 Raman spectra taken from the unused cutting inserts are given in Fig. 6, comparatively. As seen in Fig. 6, clear differences were present between the Raman spectra of the worn and unworn cutting inserts. The 672 cm^{-1} band emerging after wear indicates TiC formation [34], while the 635 cm^{-1} and 454 cm^{-1} bands observed before wear shows TiCN formation [24]. The band observed at 561 cm^{-1} belongs to the TiCN coating of the cutting insert. This band was observed at 568 cm^{-1} in a TiCN thin film study by Constable et al.[23] As a result of wear, the Al_2O_3 vibrational bands were also decreased. As seen in Fig. 7, in the mean Raman spectrum of the unused cutting inserts, the bands observed at 506 (A_{2u}) and 582 (E_g) cm^{-1} were assigned to the Al_2O_3 vibrational modes.[35–37] For the Raman spectrum of single crystal Al_2O_3[35], the observed 578 cm^{-1} Raman band was assigned to E_g internal mode, and for γ-Al_2O_3, the observed 512 and 578 cm^{-1} Raman bands were assigned to A_{2u} and E_g phonon modes, respectively.[36] In a 2004 study by Barshiliaa and Rajam on Al_2O_3, these bands were observed at 418 and 993 cm^{-1},[38] while in the study on α-Al_2O_3 and γ-Al_2O_3, these bands were observed at 416 and 507 cm^{-1}[39].

The second-order acoustic (2A) peak of TiN at 454 cm^{-1} and longitudinal optical (LO) peaks of TiN at 506, 561, 582 cm^{-1}[40] disappears as a result of worn effect, in the same way, the peak at 672 cm^{-1} of TiC gets more pronounced. The Al_2O_3 bands at 635 and 752 cm^{-1}, observed in the Raman spectrum of unused cutting insert, were diminished by worn effect. The contribution of the out-of-plane bending mode of graphitic carbon domains to 752 cm^{-1} band cannot be neglected.[41]

Fig. 7 shows the 400–700 cm^{-1} region of the mean Raman spectra of the unworn samples together with its second-derivative profile. The mean Raman spectrum of the worn samples is included for comparison. The mean Raman spectra subjected to two-point linear baseline

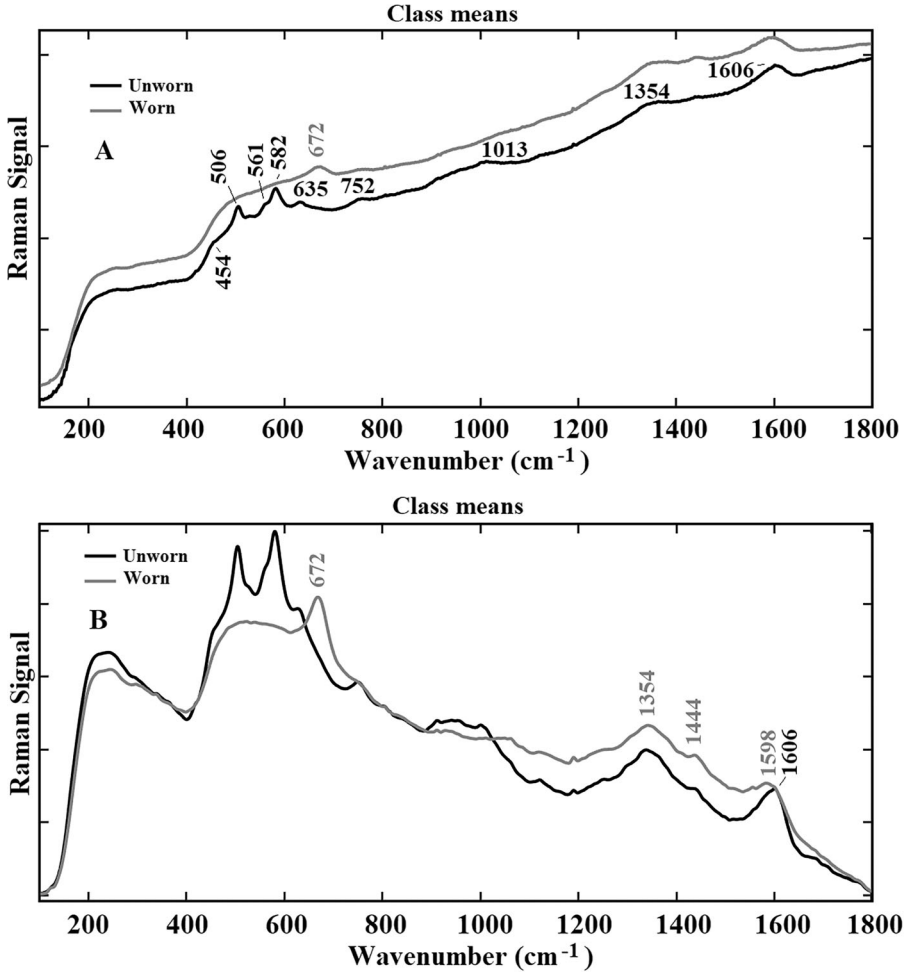

Figure 6. The mean Raman spectra of unworn (black) and worn (grey) cutting inserts. (A) The averaged original spectra and (B) the averaged pretreated (with rubberband baseline correction and vector normalization) Raman spectra.

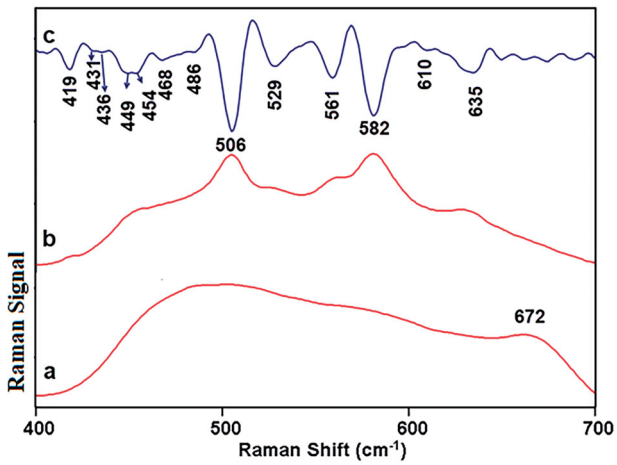

Figure 7. The 400–700 cm^{-1} region of mean Raman spectrum of worn (a) unworn (b) samples and the second-derivative profile of the mean Raman spectrum of unworn samples (c).

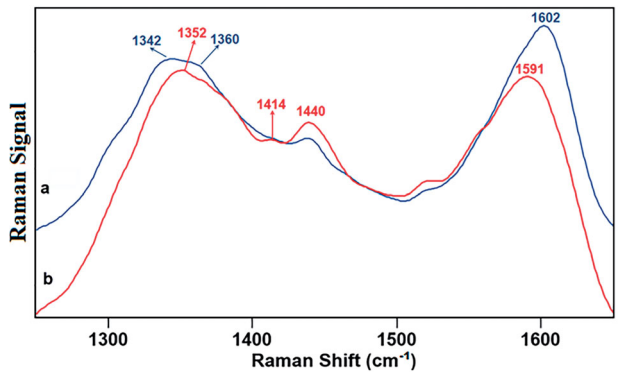

Figure 8. The 1260–1665 cm^{-1} region of the mean Raman spectra of unworn (a) and worn (b) samples.

correction between 400 and 700 cm^{-1}. From the second derivative of the mean Raman spectrum of unused (unworn) cutting inserts, the 419, 431, and 449 cm^{-1} bands of Al_2O_3[36,37] and 436, 468, 486, 529, and 610 cm^{-1} bands of TiN were additionally revealed.[40]

Another noticeable difference when comparing the Raman spectra of the samples before and after wear is the relative intensity alteration of the disordered carbon (D band, ca. 1350 cm^{-1})

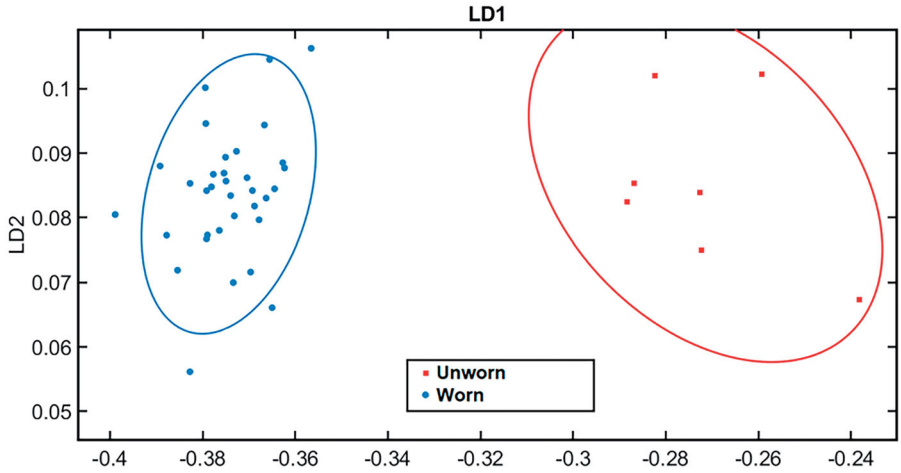

Figure 9. 2D scores plot, mapping LD1 along LD2, containing ellipse walls encapsulating 90% of the data points. The pretreated (rubberband baseline corrected, vector normalized) each Raman spectrum is shown as a point within the ellipses.

band to the graphitic sp^2 bonded carbon (G band, around 1590–1600 cm^{-1}) band. The 1260–1665 cm^{-1} region of the two-point linear baseline corrected mean Raman spectra of the worn and unworn samples were shown comparatively in Fig. 8.

Intensification of the disordered carbon band compared to the graphite band and the frequency shifts or disappearance of some other bands, indicating that the disordered carbon content of the coating has relatively increased due to wear.[36,42] The decrease in intensity of graphitic carbon band (I_G) probably due to micro-chipping, as a result of worn. In the study conducted by Abedi et al.,[43] the changes caused by annealing of the TiSiCN nanocomposite coatings were examined with the Raman Spectroscopy technique and an increase in the ratio of the intensity of the D (I_D) band to the intensity of the G band (I_G), was interpreted as an indicator for decrease in the degree of crystallinity of the carbon phase.[43]

Multivariate statistical analysis

To determine the similarities and dissimilarities between the worn and unworn $TiCN/Al_2O_3/TiN$-coated cutting inserts, multivariate statistical analysis was performed. PCA followed by LDA were applied on the 41 pretreated Raman spectra (see Fig. 6B). PCA is mostly used as a data reduction tool. PCA minimizes the variance within classes to account for the heterogeneity of similar tissue samples. Also, LDA maximizes the variance between classes, allowing for diagnostic differences to be noticed. The combination of the PCA with LDA (PCA-LDA) is a powerful tool to determine similarities and dissimilarities of the samples. PCA-LDA analysis was performed using the IRootlab toolbox[28] for MATLAB.

Fig. 9 shows two-dimensional (2D) score plot mapping LD1 along LD2. The 2D graph shows clear separation of the first (unworn) and second (worn) groups across LD1 and LD2. Moreover, the one-dimensional (1D) scores plot, for LD1 and LD2, given in Fig. 10 shows a distinct linear separation between groups 1 (unworn) and 2 (worn) along LD1. The median stage scores shift from −0.27 up to −0.37, in going group 1 to group 2.

The loading plot shows the decisive peaks representing differences between the two groups. The cluster vector loading plot of group 2 (worn) samples was drawn by considering the group 1 (unworn) samples as a reference, to reveal the distinct peaks associated with the wear effect. Fig. 11 shows the cluster vector loading plot of group 2 samples, when compared with coefficient 0 (group 1), and the main Raman wave numbers separating group 2 from group 1 are clearly seen.

Conclusions

Tool wear characteristics in CVD $TiCN/Al_2O_3/TiN$ multilayer-coated insert during milling of

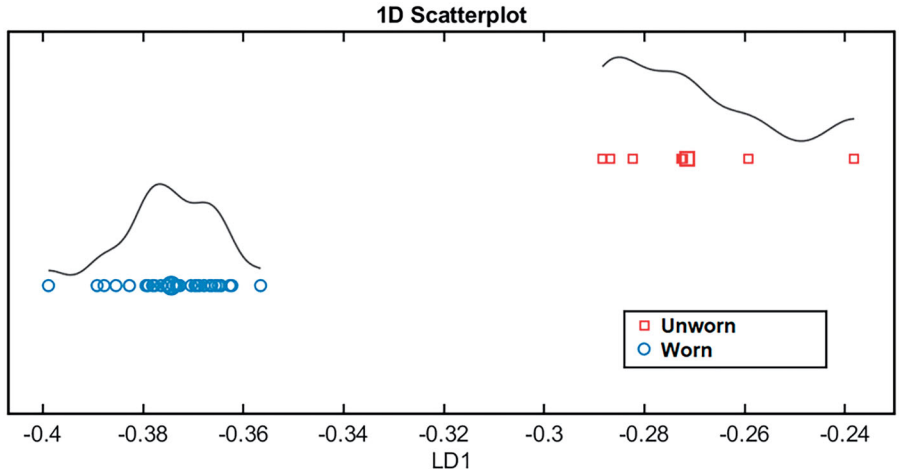

Figure 10. The 1D scores plot along LD1. Spectra are separated into two groups; worn and unworn (groups; 1 and 2) and show a distinct linear separation along LD1.

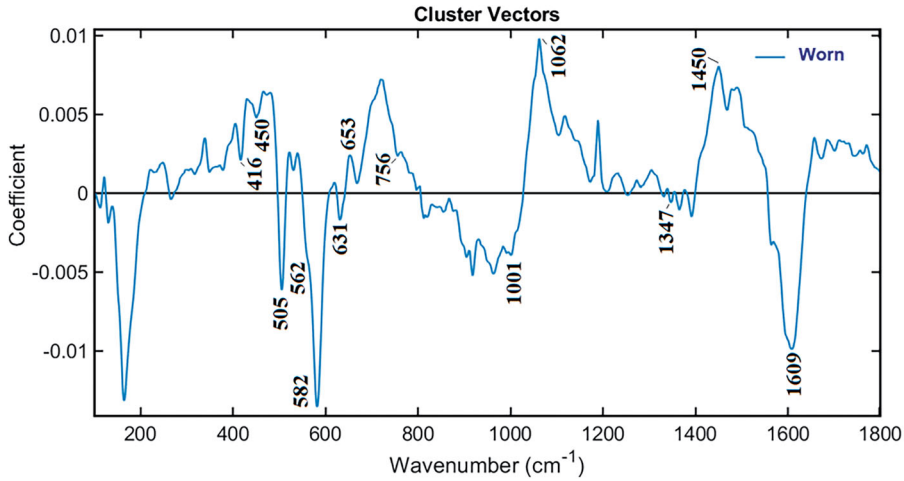

Figure 11. The cluster vector loading plot of group 2 (worn) samples, when compared to group 1 (coefficient 0), shows the distinct wavenumbers associated with wear effect.

AISI 4140 steel have been studied by SEM observation and Raman analysis. The following conclusions have been drawn:

- This study mainly covers a basic research on tool wear and tool life in terms of flank wear. Tool life was determined at 0.5 mm flank wear of the cutting insert.
- It was observed that adhesion wear and abrasion wear were the main wear mechanisms at all cutting inserts used in the study.
- In this study, changes in molecular level due to wear of TiCN/Al2O3/TiN-coated cutting inserts were investigated. It was shown that as the wear effect TiN and Al2O3 bands decreased, whereas TiC band increased. The observed decrease in the Raman intensities of the TiN and Al2O3 bands is due to micro-chipping. It was determined that the relative density of the irregular carbon (D band) band to the graphitic sp2 bonded carbon (G band) band increased as a result of wear. This result is an indication of the increase in amorphous carbon content because of wear. The multivariate analysis enabled us to make district separation between used and unused cutting inserts.
- A standard procedure is needed to determine the machinability of cutting tool-workpiece components. This procedure should also be the basis for developing a standard for determining the life and performance of cutting tools. We think this study will help.

Disclosure statement

No potential conflict of interest was reported by the author(s).

Funding

This work was supported by the Scientific Research Projects Coordination Unit of Istanbul University (ÖNAP-2423).

ORCID

Sefa Celik http://orcid.org/0000-0001-6216-1297
Nuray Bekoz Ullen http://orcid.org/0000-0003-2705-2559
Sevim Akyuz http://orcid.org/0000-0003-3313-6927
Aysen E. Ozel http://orcid.org/0000-0002-8680-8830

References

[1] Sarıkaya, M.; Gupta, M. K.; Tomaz, I.; Pimenov, D. Y.; Kuntoğlu, M.; Khanna, N.; Yildirim, C. V.; Krolczyk, G. M. A State-of-the-Art Review on Tool Wear and Surface Integrity Characteristics in Machining of Superalloys. *CIRP Journal of Manufacturing Science and Technology* **2021**, *35*, 624–658. DOI: 10.1016/j.cirpj.2021.08.005.

[2] Khan, T.; Broderick, M.; Taylor, C. M. Investigating the Industrial Impact of Hydraulic Oil Contamination on Tool Wear During Machining and the Development of a Novel Quantification Methodology. *The International Journal of Advanced Manufacturing Technology* **2021**, *112*(1-2), 589–600. DOI: 10.1007/s00170-020-06370-y.

[3] Badiger, P. V.; Desai, V.; Ramesh, M. R.; Prajwala, B. K.; Raveendra, K. Effect of Cutting Parameters on Tool Wear, Cutting Force and Surface Roughness in Machining of MDN431 Alloy Using Al and Fe Coated Tools. *Materials Research Express* **2018**, *6*(1), 016401. DOI: 10.1088/2053-1591/aae2a3.

[4] Badiger, P.; V; Desai, V.; Ramesh, M. R.; Prajwala, B. K.; Raveendra, K. Cutting Forces, Surface Roughness and Tool Wear Quality Assessment Using ANN and PSO Approach During Machining of MDN431 With TiN/AlN-Coated Cutting Tool. *Arabian Journal for Science and Engineering* **2019**, *44* (9), 7465–7477. DOI: 10.1007/s13369-019-03783-0.

[5] Bayraktar, Ş.; Hekimoğlu, A. P. Effect of Zinc Content and Cutting Tool Coating on the Machinability of the Al-(5–35) Zn Alloys. *Metals and Materials International* **2020**, *26*(4), 477–490. DOI: 10.1007/s12540-019-00582-y.

[6] Davim, J. P. *Surface Integrity in Machining*; Springer: London, 2010.

[7] Childs, T. H.; Maekawa, K.; Obikawa, T.; Yamane, Y. *Metal Machining: Theory and Applications*. Oxford, England: Butterworth-Heinemann, 2000.

[8] Dhar, N. R.; Paul, S.; Chattopadhyay, A. B. Machining of AISI 4140 Steel Under Cryogenic Cooling—Tool Wear, Surface Roughness and Dimensional Deviation. *Journal of Materials Processing Technology* **2002**, *123*(3), 483–489. DOI: 10.1016/S0924-0136(02)00134-6.

[9] Hadad, M.; Sadeghi, B. Minimum Quantity Lubrication-MQL Turning of AISI 4140 Steel Alloy. *Journal of Cleaner Production* **2013**, *54*, 332–343. DOI: 10.1016/j.jclepro.2013.05.011.

[10] Harto, B.; Umroh, B.; Darianto, D. Study on the CBN Tool Wear Mechanism on Dry High-Rate Turning Process for AISI 4140. *Journal of Mechanical Engineering, Manufactures, Materials and ENERGY* **2018**, *2*(1), 20–26. DOI: 10.31289/jmemme.v2i1.1654.

[11] Kaynak, Y.; Gharibi, A. Progressive Tool Wear in Cryogenic Machining: The Effect of Liquid Nitrogen and Carbon Dioxide. *Journal of Manufacturing and Materials Processing* **2018**, *2*(2), 31. DOI: 10.3390/jmmp2020031.

[12] Arrazola, P. J.; Arriola, I.; Davies, M. A.; Cooke, A. L.; Dutterer, B. S. The Effect of Machinability on Thermal Fields in Orthogonal Cutting of AISI 4140 Steel. *CIRP Annals* **2008**, *57*(1), 65–68. DOI: 10.1016/j.cirp.2008.03.139.

[13] Khrais, S. K.; Lin, Y. J. Wear Mechanisms and Tool Performance of TiAlN PVD Coated Inserts During Machining of AISI 4140 Steel. *Wear* **2007**, *262*(1-2), 64–69. DOI: 10.1016/j.wear.2006.03.052.

[14] Talib, R. J.; Ariff, H. M.; Toff, M. R. M. Wear Mechanism of TiN, TiAlN and TiCN Coated Drills During Drilling of Carbon Steel. *Journal of Physical Science* **2007**, *18*(1), 75–85.

[15] Dreiling, I.; Haug, A.; Holzschuh, H.; Chasse, T. Raman Spectroscopy as a Tool to Study Cubic Ti–C–N CVD Coatings. *Surface and Coatings Technology* **2009**, *204*(6-7), 1008–1012. DOI: 10.1016/j.surfcoat.2009.05.029.

[16] García-González, L.; Garnica-Romo, M. G.; Hernández-Torres, J.; Espinoza-Beltrán, F. J. A Study of TiAlN Coatings Prepared by RF Co-Sputtering. *Brazilian Journal of Chemical Engineering* **2007**, *24*(2), 249–257. DOI: 10.1590/S0104-66322007000200009.

[17] Blanpain, B.; Franck, M.; Mohrbacher, H.; Vancoille, E.; Celis, J. P.; Roos, J. R. Micro-Raman Spectroscopy for the Characterization of Wear Induced Surface Modifications on Hard Coatings. In *Thin Films in Tribology*; Dowson, D.; Taylor, C. M.; Childs, T. H. C.; Godet, M.; Dalmaz, G., Eds.; Academic Press; Elsevier: Amsterdam, The Netherlands. 1993, 623–630.

[18] Vancoille, E.; Blanpain, B.; Xingpu, Y.; Celis, J. P.; Roos, J. R. Tribo-Oxidation of a TiN Coating Sliding Against Corundum. *Journal of Materials Research* **1994**, *9*(4), 992–998. DOI: 10.1557/JMR.1994.0992.

[19] Murari, N.; Sergo, V.; Pezzotti, G.; Katagiri, G.; Meriani, S.; Nishida, T. Raman Piezo-Spectroscopic Behavior of Aluminum Nitride. *Applied Spectroscopy* **1997**, *51*(11), 1761–1765. DOI: 10.1366/0003702971939497.

[20] Begun, G. M.; Bamberger, C. E. Raman Spectroscopic Observation of Laser-Induced Oxidation of Transition-Metal Borides, Carbides, and Nitrides. *Applied Spectroscopy* **1989**, *43*(1), 134–138. DOI: 10.1366/0003702894201914.

[21] Franck, M.; Celis, J. P.; Roos, J. R. Microprobe Raman Spectroscopy of TiN Coatings Oxidized by Solar Beam Heat Treatment. *Journal of Materials Research* **1995**, *10*(1), 119–125. DOI: 10.1557/JMR.1995.0119.

[22] Chowdhury, R.; Vispute, R. D.; Jagannadham, K.; Narayan, J. Characteristics of Titanium Nitride Films Grown by Pulsed Laser Deposition. *Journal of Materials Research* **1996**, *11*(6), 1458–1469. DOI: 10.1557/JMR.1996.0182.

[23] Constable, C. P.; Yarwood, J.; Münz, W. D. Raman Microscopic Studies of PVD Hard Coatings. *Surface and Coatings Technology* **1999**, *116-119*, 155–159. DOI: 10.1016/S0257-8972(99)00072-9.

[24] Badiger, P.; Desai, V.; Ramesh, M. R.; Joladarashi, S.; Gourkar, H. Tribological Behaviour of Monolayer and Multilayer Ti-Based Thin Solid Films Deposited on Alloy Steel. *Materials Research Express* **2018**, *6*(2), 026419. DOI: 10.1088/2053-1591/aaef6d.

[25] Badiger, P.; Desai, V.; Ramesh, M. R. Development and Characterization of Ti/TiC/TiN Coatings by Cathodic Arc Evaporation Technique. *Transactions of the Indian Institute of Metals* **2017**, *70*(9), 2459–2464. DOI: 10.1007/s12666-017-1107-9.

[26] Sandvik Product Catalogue, 2019, Workpiece materials. Document Moved [online]. Copyright © Sandvik Coromant. https://www.sandvik.coromant.com/engb/knowledge/materials/pages/workpiece-materials.aspx (accessed Dec 10, 2021]).

[27] Esbensen, K. H. *Multivare Data Analysis-in Practice*; CAMO Process AS: Norway, 2004, 19–72.

[28] Trevisan, J.; Angelov, P. P.; Scott, A. D.; Carmichael, P. L.; Martin, F. L. IRootLab: A Free and Open-Source MATLAB Toolbox for Vibrational Biospectroscopy Data Analysis. *Bioinformatics (Oxford, England)* **2013**, *29*(8), 1095–1097. DOI: 10.1093/bioinformatics/btt084.

[29] Barry, J.; Byrne, G. Cutting Tool Wear in the Machining of Hardened Steels: Part I: Alumina/TiC Cutting Tool Wear. *Wear* **2001**, *247*(2), 139–151. DOI: 10.1016/S0043-1648(00)00531-7.

[30] Hu, J.; Chou, Y. K. Characterizations of Cutting Tool Flank Wear-Land Contact. *Wear* **2007**, *263*(7-12), 1454–1458. DOI: 10.1016/j.wear.2007.01.080.

[31] Wang, J.; Huang, C. Z.; Song, W. G. The Effect of Tool Flank Wear on the Orthogonal Cutting Process and Its Practical Implications. *Journal of Materials Processing Technology* **2003**, *142*(2), 338–346. DOI: 10.1016/S0924-0136(03)00604-6.

[32] Hoier, P.; Klement, U.; Alagan, N. T.; Beno, T.; Wretland, A. Flank Wear Characteristics of WC-Co Tools When Turning Alloy 718 With High-Pressure Coolant Supply. *Journal of Manufacturing Processes* **2017**, *30*, 116–123. DOI: 10.1016/j.jmapro.2017.09.017.

[33] Kelly, J. G.; Trevisan, J.; Scott, A. D.; Carmichael, P. L.; Pollock, H. M.; Martin-Hirsch, P. L.; Martin, F. L. Biospectroscopy to Metabolically Profile Biomolecular Structure: A Multistage Approach Linking Computational Analysis With Biomarkers. *Journal of Proteome Research* **2011**, *10*(4), 1437–1448. DOI: 10.1021/pr101067u.

[34] Qi, Q.; Zhang, W. Z.; Shi, L. Q.; Zhang, W. Y.; Zhang, W.; Zhang, B. Preparation of Single-Crystal TiC (111) by Radio Frequency Magnetron Sputtering at Low Temperature. *Thin Solid Films.* **2012**, *520*(23), 6882–6887. DOI: 10.1016/j.tsf.2012.07.040.

[35] Li, P. G.; Lei, M.; Tang, W. H. Raman and Photoluminescence Properties of α-Al2O3 Microcones With Hierarchical and Repetitive Superstructure. *Materials Letters* **2010**, *64*(2), 161–163. DOI: 10.1016/j.matlet.2009.10.032.

[36] Liu, Y.; Cheng, B.; Wang, K. K.; Ling, G. P.; Cai, J.; Song, C. L.; Han, G. R. Study of Raman Spectra for γ-Al2O3 Models by Using First-Principles Method. *Solid State Communications* **2014**, *178*, 16–22. DOI: 10.1016/j.ssc.2013.09.030.

[37] Porto, S. P. S.; Krishnan, R. S. Raman Effect of Corundum. *The Journal of Chemical Physics* **1967**, *47*(3), 1009–1012. DOI: 10.1063/1.1711980.

[38] Barshilia, H. C.; Rajam, K. S. Raman Spectroscopy Studies on the Thermal Stability of TiN, CrN, TiAlN Coatings and Nanolayered TiN/CrN, TiAlN/CrN Multilayer Coatings. *Journal of Materials Research* **2004**, *19*(11), 3196–3205. DOI: 10.1557/JMR.2004.0444.

[39] Boratto, M. H.; de Andrade Scalvi, L. V. Deposition of Al2O3 by Resistive Evaporation and Thermal Oxidation of Al to be Applied as a Transparent FET Insulating Layer. *Ceramics International* **2014**, *40*(2), 3785–3791. DOI: 10.1016/j.ceramint.2013.09.041.

[40] Saoula, N.; Djerourou, S.; Yahiaoui, K.; Henda, K.; Kesri, R.; Erasmus, R. M.; Comins, J. D. Study of the Deposition of Ti/TiN Multilayers by Magnetron Sputtering. *Surface and Interface Analysis* **2010**, *42*(6-7), 1176–1179. DOI: 10.1002/sia.3299.

[41] Chen, R.; Tu, J. P.; Liu, D. G.; Mai, Y. J.; Gu, C. D. Microstructure, Mechanical and Tribological Properties of TiCN Nanocomposite Films Deposited by DC Magnetron Sputtering. *Surface and Coatings Technology* **2011**, *205*(21-22), 5228–5234. DOI: 10.1016/j.surfcoat.2011.05.034.

[42] Papadimitriou, D.; Roupakas, G.; Dimitriadis, C. A.; Logothetidis, S. Raman Scattering and

Photoluminescence of Nitrogenated Amorphous Carbon Films. *Journal of Applied Physics* **2002**, *92*(2), 870–875. DOI: 10.1063/1.1488251.

[43] Abedi, M.; Abdollah-Zadeh, A.; Bestetti, M.; Vicenzo, A.; Serafini, A.; Movassagh-Alanagh, F. The Effects of Phase Transformation on the Structure and Mechanical Properties of TiSiCN Nanocomposite Coatings Deposited by PECVD Method. *Applied Surface Science* **2018**, *444*, 377–386. DOI: 10.1016/j.apsusc.2018.02.263.